


Retarding spreading of surfactant drops on solid surfaces: Interplay between the Marangoni effect and capillary flows

Parisa Bazazi  and S. Hossein Hejazi

Department of Chemical and Petroleum Engineering, University of Calgary, Calgary, Alberta, Canada T2N 1N4



(Received 5 November 2019; accepted 5 August 2020; published 27 August 2020)

The characteristics of an aqueous drop spreading on a solid surface are the keys to many deposition processes, including coating, printing, enhanced oil production, and surfactant replacement therapies. It is generally believed that the addition of surface-active materials increases the rate of the drop spreading. We report on an unexpected phenomenon whereby the initial spread of surfactant drops is impeded by the Marangoni stresses, resulting in a large increase in the total spreading time. This is demonstrated by an experimental study of the early-time regimes of surfactant-laden drops spreading on a hydrophilic solid surface, submerged in a second immiscible viscous liquid. Remarkably, we find that the surfactants delay the initial fast motion of the three-phase contact lines. The nonuniform distribution of the surfactants at the interface generates the Marangoni stresses before the drop-solid contact that suppresses the film drainage and the expansion of the droplet. Surfactant solutions with 0.1 and 1 critical micelle concentrations wet the surface, with their radius growing according to $r \sim t^{0.5}$ for very short timescales, as opposed to the viscous regime for which $r \sim t$. Our research can provide a guideline for the design of systems with controllable and desirable wetting dynamics.

DOI: [10.1103/PhysRevFluids.5.084006](https://doi.org/10.1103/PhysRevFluids.5.084006)

I. INTRODUCTION

Spontaneous wetting of a solid surface and removal of one fluid from it by a second immiscible fluid occur in many natural and industrial processes, ranging from enhanced oil recovery to lubrication, printing, coating, and drug delivery [1–6]. The dynamics of surface wetting depends on the nature of the substrate, as well as the properties of the fluid droplets and the surrounding fluid phases [1,7]. After a fluid droplet touches a surface in clean systems, such as those without surface-active molecules, its spreading evolves through various regimes that are all characterized by the growth of the wetted radius r with the time t by a power law of the general form $r \sim t^\alpha$. The out-of-balance contact angle triggers spontaneous spreading where the capillary force that results from a highly curved fluid-fluid interface at the contact point drives the drop towards its final semispherical shape at the equilibrium contact angle. The balance between capillary and viscous forces determines the early-time spreading dynamics in clean systems, characterized by a droplet radius that grows linearly with the time, $r \sim t$ [8–11]. The wetting finally evolves to a state in which it follows the power law $r \sim t^{1/10}$, representing the late-time Tanner regime [12]. In addition to the hydrodynamic point of view, one may consider the molecular kinetic theory to describe the drop spreading, which has been successfully used to explain the late-time spreading dynamics in air and liquid mediums [13–18].

In most practical cases, however, wetting systems are not clean and surface-active materials are present, either in the fluids or on the solids [19–23]. The interface evolution in such systems may be accompanied by the surfactants' concentration gradient [24,25], which results in the transport

of the surfactants from the bulk to the newly formed interface, generating local variations in interfacial tension (IFT) and, consequently, giving rise to the Marangoni flows. The physics of droplet spreading on a solid substrate is analogous to the coalescence dynamics of two spherical drops with identical properties, for which it is known that the presence of surfactants can increase the required time for the drainage of a thin film formed between the two drops, hence delaying, or preventing altogether, the onset of coalescence [26–29]. Likewise, in the case of surfactant droplets spreading on solids, the nonuniform surfactant distribution at the interface influences the spreading rate by altering the surface flow, the droplet’s shape, and the balance of the forces at the contact line. Thus, the spreading rate may be enhanced or diminished relative to the clean interface.

Past spreading experiments characterized mainly the role of surfactants, in terms of superspreaders, on the final wetted area over timescales on the order of seconds or minutes. It has been reported that superspreaders wet the surface with their radius growing according to $r \sim t$, as opposed to $r \sim t^{0.1}$ predicted by the late-time Tanner regime [20]. The linear spreading dynamic of superspreaders is due to the Marangoni forces and the surfactant-free zone in the vicinity of the contact line [30]. Many studies have reported increased wetted areas due to the contact angle changes when surfactants, such as sodium dodecyl sulfate (SDS), hexadecyltrimethylammonium bromide (CTAB), or trisiloxane (silicon-based surfactants), are present [19,21,31–33]. On the other hand, studies on the early-time dynamics of surfactant droplets spreading on solid substrates are scarce and limited to a few experiments, carried out in an ambient inviscid fluid, air. von Bahr *et al.* [34] investigated the spreading of water and surfactant drops of polyethylene glycol alkyl ether C14E6 in an environment that had been presaturated with the vapor of the same liquid. For both water and surfactant drops, an initial spreading process with a power-law growth, $r \sim t^{0.5}$, was reported. Such a fast spreading slowed down to a second regime after about 30 ms for the surfactant drop. In a similar study, Wang *et al.* [21] investigated the early-time spreading of water drops containing the ionic surfactants SDS and CTAB, as well as nonionic trisiloxane surfactants, representing superspreaders, when deposited on a hydrophobic substrate. All the surfactant drops exhibited an early-time spreading regime that is controlled by the balance between inertia and capillary forces, characterized by a power-law growth of the radius with the time with an exponent of $\alpha \simeq 0.3$ – 0.45 . Such a regime lasts for times less than 12 ms for SDS and CTAB, until equilibrium is reached [21].

Unlike the coalescence dynamics of surfactant drops [26–29], the two aforementioned studies exhibit little differences in the early-time spreading regime of water and surfactant drops. The fact that von Bahr *et al.* [34] and Wang *et al.* [21] used side-view images may have affected capturing the early-time wetting dynamics. Indeed, Eddi *et al.* [8] showed that the side-view images of the drop spreading suffer from the merging between the drop image with its own optical reflection on the glass substrate. Thus, the measured spreading radius r may have been overestimated. In contrast, the bottom-view imaging improves highly the spatial resolution and provides an accurate estimation of the wetted area [8]. The discrepancy between the side- and bottom-view images vanished when the wetted radius grew to a size on the order of a few hundred microns, $r \sim 300 \mu\text{m}$ [8]. Moreover, at the time of contact, liquid drops spread very fast on solids when the surrounding fluid is air. Thus, it is possible to miss the subtle interactions between the surface tension-driven flows and the three-phase contact-line movement.

The early-stage characteristics of a surfactant-laden droplet spreading on solid surfaces is utilized to improve the performance of many liquid-fluid-solid systems containing surface-active materials, such as self-cleaning surfaces, drug delivery, enhanced oil and gas production, CO₂ sequestration, coating, and three-dimensional printing. Obtaining accurate records of the early-time wetting process is, however, a difficult problem and requires bottom-view imaging with a coupled microscope and high-speed camera in order to achieve high spatiotemporal resolutions. In this article we employ such an imaging setup for a liquid-liquid spreading system to unravel the physics behind the wetting by surfactant drops. The presence of a viscous bulk phase can considerably slow down the spreading dynamics, hence providing enough time to capture the delicate role of the Marangoni flows on the dynamics of the early-time stage of wetting.

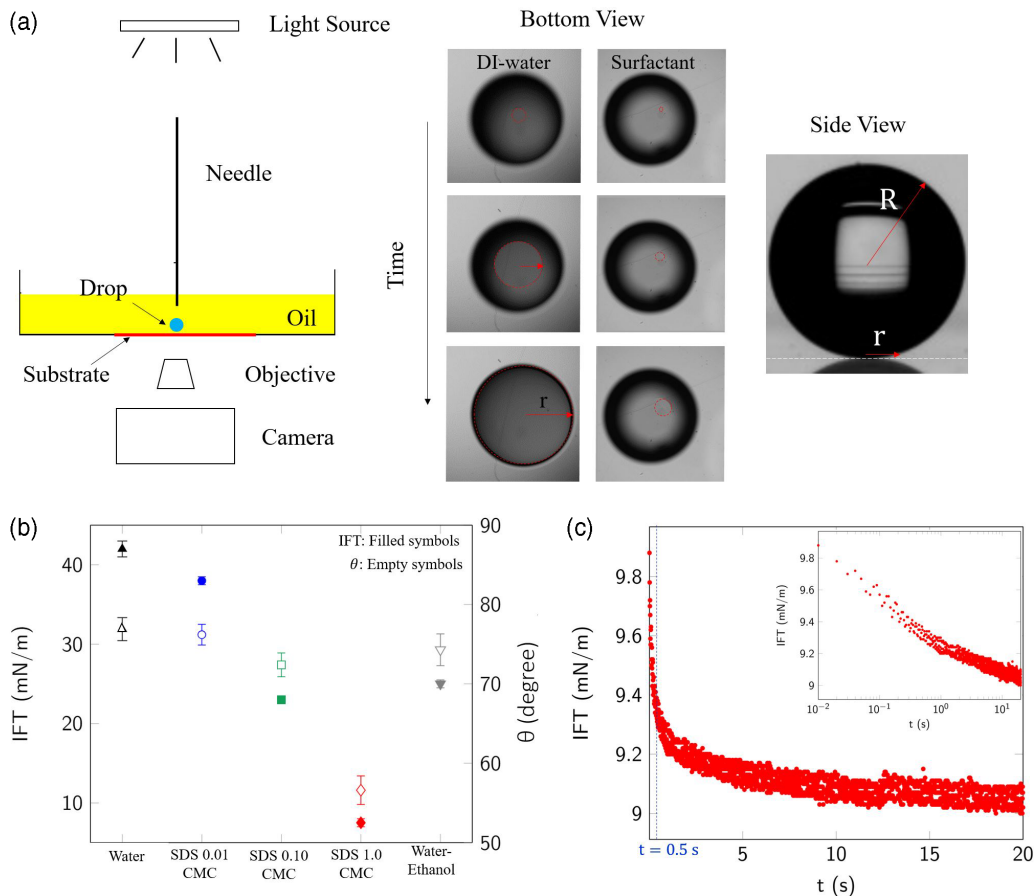


FIG. 1. (a) Schematic of the experimental setup. The bottom-view images were used for measuring the radius $r(t)$ of the spreading area, and side-view images were used for detecting the drop shape. (b) The IFT and contact angle values of the samples. Triangles, spheres, squares, and inverted triangles show the data for water, SDS 0.1 CMC, SDS 1 CMC, and the water-ethanol mixture, respectively. Solid and empty symbols represent the IFT and the contact angle data. (c) Dynamic IFT of the 1 CMC solution of SDS.

II. EXPERIMENTS

The experimental setup consists of a Petri dish placed on the stage of an inverted Ti2 Nikon microscope, coupled with a high-speed camera (Zyla 4.2 158 PLUS sCMOS), as sketched in Fig. 1(a). A glass slide with known contact angle is placed at the bottom of the Petri dish filled with a viscous oil. An aqueous drop with a fixed volume of $2 \mu\text{l}$ and a radius of $R = 780 \mu\text{m}$ is released from a micropipette, placed about 7 mm above the glass slide. The droplet descends and spreads on the glass surface. The bottom-view images of the drops are captured by the camera at 50 fps and a resolution of $1.6 \mu\text{m}/\text{pixel}$, resulting in the history growth of the droplet's radius $r(t)$. Each set of experiments is repeated at least ten times. Error bars represent the standard deviation of ten measurements. We also capture the side-view images with an unsynchronized camera, installed on the DSA 100 setup, in order to monitor the drop's shape with a frequency of 300 fps and a resolution of $9 \mu\text{m}/\text{pixel}$.

We used a viscous oil, Drakeol 35 (with viscosity $\mu_o = 178 \text{ mPa s}$ and density $\rho = 867 \text{ kg/m}^3$), and untreated hydrophilic glass slides (VWR, VistaVision) as received. Distilled water (with density $\rho = 997 \text{ kg/m}^3$) was used for the baseline experiments without the surfactant, and SDS solutions

(Sigma Aldrich; with $\rho = 997 \text{ kg/m}^3$) with the concentrations of 0.01, 0.1, and 1 critical micelle concentration (CMC) were used in the experiments with the surfactants. SDS is an anionic surfactant with a CMC of 8.3 mM and a molecular weight of 288.372 g/mol. For one set of experiments, ethanol (97.8% wt., Fisher scientific) was added to the water at 30 vol%, resulting in a solution with an IFT similar to that of the 0.1 CMC SDS solution. We assumed that all the aqueous drops have the same viscosity of the water (with viscosity $\mu_w = 1 \text{ mPa s}$). We measured the oil-aqueous phase IFT and the contact angle using a drop-shape analyzer (DSA 100, Kruss). The IFT and contact angle data for the clean system (distilled water and oil) were $42.0 \pm 1.0 \text{ mN/m}$ and $76.9 \pm 1.6^\circ$, respectively, and are decreasing functions of the SDS concentration, as depicted in Fig. 1(b), which represents the equilibrium data collected after 10^3 s . In order to establish the timescale for the adsorption of the SDS, we also measured the IFT as a function of time. Figure 1(c) presents the data for a 1 CMC solution, which exhibit fast reduction from 10.0 to 9.3 mN/m over the first 500 ms.

III. RESULTS AND DISCUSSION

The drop settled under gravity until it came to an apparent resting position on the solid. A thin film of the homophase formed and thinned out until it ruptured under the action of the attractive forces [35]. An axisymmetric contact ring, i.e., the wetted area, was formed in a ring round the rim of minimum film thickness, and further spreading was observed until the drop came to rest in an equilibrium state dictated solely by the contact angle, since the Bond number, ≈ 0.7 for water and 0.41 for 1 CMC SDS solution, was small. We define the rupture time as $t = 0$ and the drop resting time (before the rupture when the drop settles) as Δt_r .

We first discuss the spreading rates. The measured radii $r(t)$ of the area wetted by the drop are shown in Fig. 2(a) for pure water, a water-ethanol solution, and the surfactant solutions. The spreading dynamics is characterized by the power-law behavior, $r(t) \sim t^\alpha$. The apparent exponent α was estimated by $\alpha = d \log(r)/d \log(t)$ from experimental data; the results are plotted as a function of time in Fig. 2(b). For pure water with zero concentration of the SDS ($\sigma = 42.0 \pm 1 \text{ mN/m}$), a low concentration of the SDS (0.01 CMC with $\sigma = 38.0 \pm 0.5 \text{ mN/m}$), and the water-ethanol solution ($\sigma = 25.0 \pm 0.5 \text{ mN/m}$), there is an initial fast dynamic with an apparent exponent, $0.8 < \alpha < 1$, known as the viscous-dominated regime, for which one expects theoretically [8,9,11] to have $r \sim t$. In less than a second, the wetting process slows down and evolves to a state characterized by an exponent close to $\alpha \approx 0.1$, the aforementioned late-time Tanner regime.

Surprisingly, for higher concentrations of SDS, 0.1 CMC (with $\sigma = 23.0 \pm 0.4 \text{ mN/m}$) and 1 CMC (with $\sigma = 7.5 \pm 0.8 \text{ mN/m}$), there is very-short-time retardation in the spreading process for about 200 ms, with an apparent exponent, $0.3 < \alpha < 0.5$, which then transitions into the viscous-dominated regime with $0.7 < \alpha < 1$. The effect of the initial 200-ms retardation on the spreading process leads to an order of magnitude difference in the final spreading time. Hence, for the two higher SDS concentrations, the Tanner regime is observed after about 10 s, as compared with 1 s for water, water-ethanol, and the lower SDS concentration drops. We also considered the effect of droplet size and surrounding liquid viscosity on the initial regime of surfactant drop spreading. We found that in all cases, regardless of the size of the droplet and the oil viscosity, surfactants delayed the initial fast motion of the contact line. The transition point from the early regime with the exponent of 0.5 to the viscous regime remains intact as $\sim 0.2 \text{ s}$. The results of the effect of oil viscosity and droplet size are presented in the appendices.

We computed numerically the velocity of spreading, $U(t) = dr/dt$. The results are presented in Fig. 2(c). For water, water-ethanol, and the lower SDS concentration drops, the velocities are initially constant, followed by a sharp decline at a specific transition radius, $r = 354 \pm 13 \mu\text{m}$. Figure 2(c) shows, however, that for the higher surfactant concentrations the velocity is not constant until about $r < 20 \mu\text{m}$. This is consistent with $\alpha < 1$ for the first 200 ms, as reported in Fig. 2(b). For $r > 20 \mu\text{m}$, the spreading velocities of the two higher concentrations of the SDS remain constant, with their values being 1 order of magnitude lower than that of water, water-ethanol, and the lower

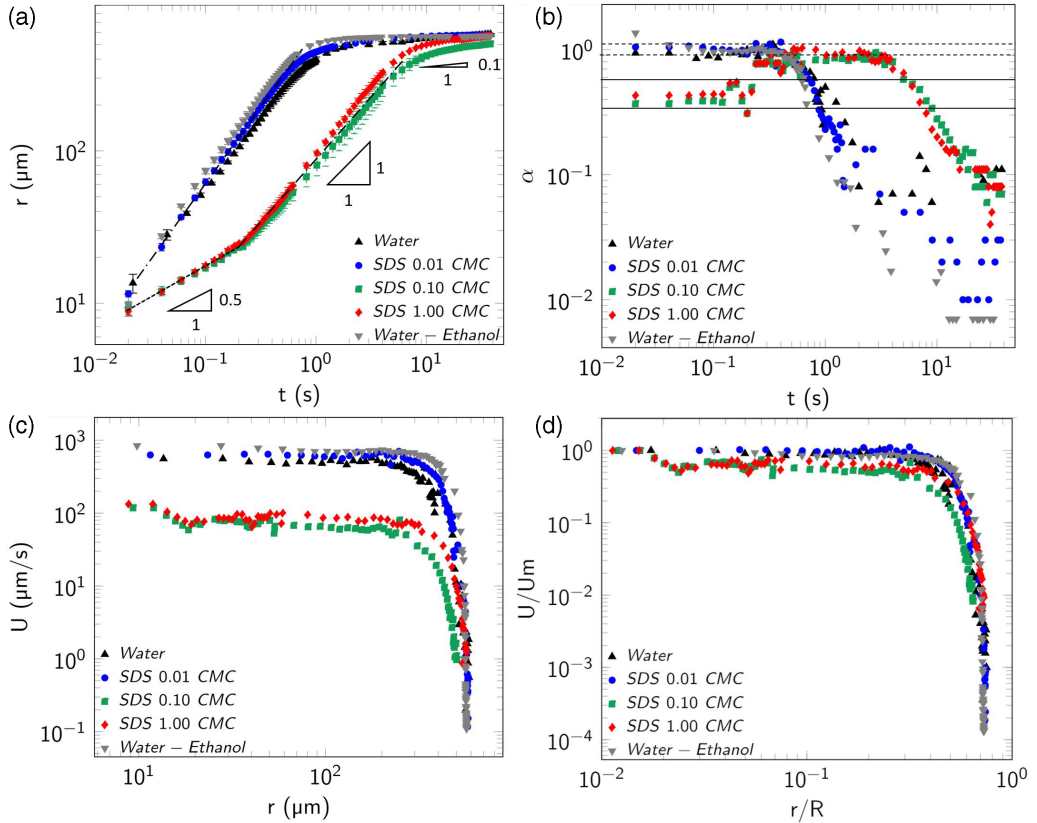


FIG. 2. (a) Evolution of radius $r(t)$ of the drop spreading at four concentrations of the surfactant, 0, 0.01, 0.1, and 1 CMC, and a mixture of water-ethanol in, respectively, black, blue, green, red, and gray on the log-log plot. (b) Evolution of the measured apparent exponent α . The zone between the solid lines represents the initial spreading regimes of water, SDS 0.01 CMC, and water-ethanol that have spreading exponents close to 1. The zone between the dashed lines shows the initial regimes of SDS 0.1 and 1 CMC that have spreading exponents close to 0.5. (c) The velocity of the three-phase contact line as a function of spreading radius r . Compared to water, the addition of the surfactant at 0.1 and 1 CMC decreases the initial spreading velocity by 1 order of magnitude. (d) Dimensionless velocity as a function of the dimensionless radius.

SDS systems. If, however, the velocities are normalized with their maximum initial values, $U(t)/U_m$, then, as Fig. 2(d) indicates, all the data collapse onto a single curve for $r/R > 0.03$.

Surfactants have at least two main effects on spreading: (i) they reduce the IFT, and (ii) they create the Marangoni stresses as a result of nonuniform surfactant distribution at the interface. The mismatch between the contact angle and its equilibrium value produces a capillary pressure gradient that drives the spreading. The capillary force $\Delta P = \sigma \bar{h}$, where \bar{h} is the curvature of the interface, is resisted by the viscous force where the corresponding capillary-driven velocity is $U_c = \sigma/\mu$. In order to analyze the effect of the IFT reduction on the spreading dynamics, the spreading of the water-ethanol drop was compared to that of the 0.1 CMC SDS solution. In the presence of surfactants, the IFT of the oil-water interface changes over time, whereas that of the water-ethanol drop remains constant (see Appendix A). Unlike the early retardation regime observed in the 0.1 CMC SDS system [Fig. 2(a)], the water-ethanol drop spreads linearly with the time, which is similar to water drops. Since both water-ethanol and 0.1 CMC SDS drops have similar equilibrium IFT values, the early retardation regime cannot be solely due to the effect of IFT reduction. The IFT across the water-ethanol drop interface is uniformly reduced, whereas the situation can be different

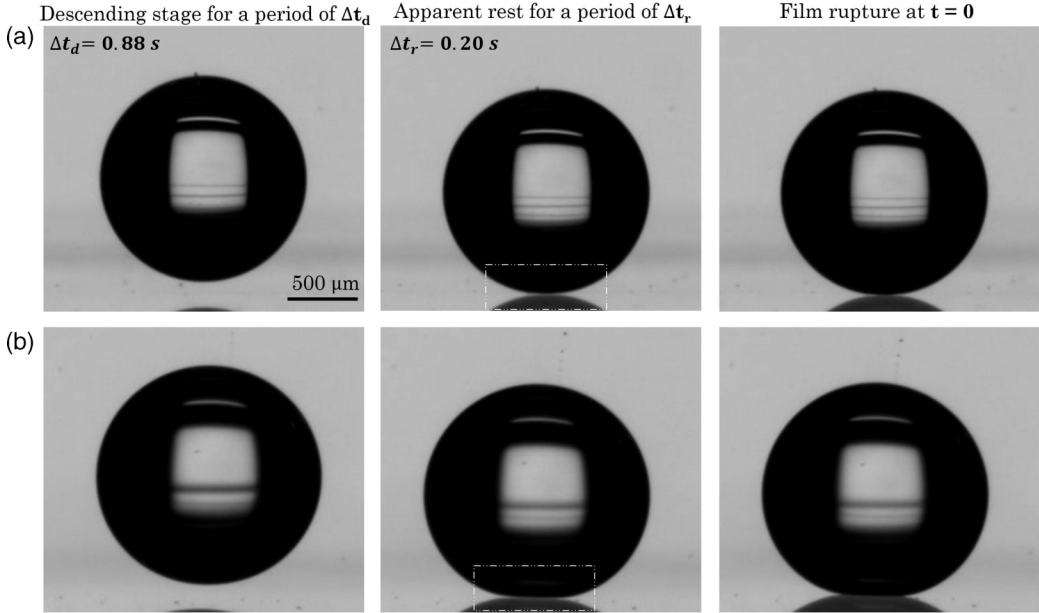


FIG. 3. Images of the drops of (a) water and (b) surfactant (with 1 CMC solution of SDS) for three stages of the process, namely, descending, resting, and the onset of spreading at the film rupture. The selected areas in the images show the flattened aqueous phase-oil film interface at the bottom of the SDS drop.

when surfactants are added to water. The distribution of the surfactant molecules at the interface can be nonuniform, hence generating the Marangoni stresses.

To unravel the role of the surfactant distribution and the consequent retardation effect, we analyzed the droplet's shapes during the settling and resting process, and collected the data for the 1 CMC SDS drop in order to contrast them with the pure water case. We define the resting time as the time elapsed from the point at which the drop comes to an apparent resting position on the solid, i.e., the end of settling process, to the point at which the film begins to rupture. Figures 3(a) and 3(b) show the side-view images of water and surfactant droplets from the released point until the onset of spreading. They show key differences in the film drainage when surfactants are present: in this case the bottom of the drop is clearly flattened. The settling time for all the drops is the same, whereas the resting time Δt_r is considerably affected by the presence of the surfactants, being about an order of magnitude larger, 1.40 ± 0.84 s, for the case of surfactant than that for water, 0.25 ± 0.07 s.

We propose a plausible mechanism for the effect of the surfactants. When the oil phase in the film between the drop and the solid surface is squeezed outwards, the surfactants on the interface are swept to the film's border. Consequently, the surfactant concentration becomes low at the center of the drop and accumulates at the film's edge. The resulting Marangoni stress opposes the outward liquid flow and generates a backflow into the film, as shown schematically in Fig. 4(b), where it is compared with the clean interface case in Fig. 4(a). The Marangoni-driven flow affects the interface curvature close to the solid surface and delays the film rupture. The deformed and extended film interface, in the presence of surfactants, can also be due to the effect of Marangoni stresses, as previously analyzed for the case of surfactant drop coalescence [21]. Dai and Leal [26] used direct numerical simulations to study the coalescence of two droplets in the presence of insoluble surfactants in the film formed between the drops. They reported that surfactants inhibit coalescence by increasing the required time for the film drainage process due to (i) the Marangoni flow within the thin film and (ii) the deformed and extended film interface into a dimple structure. The latter is a result of interface immobilization outside the film by Marangoni stresses that subsequently increase

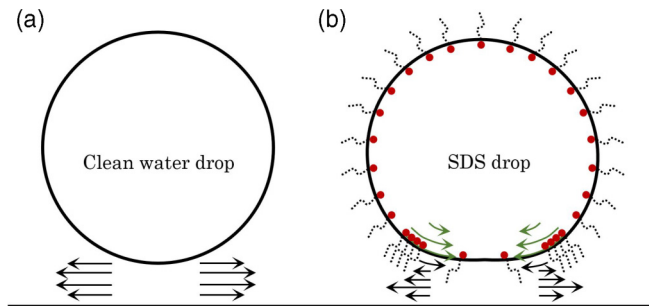


FIG. 4. (a) and (b) Effect of surfactant before the drop-solid contact. Its addition generates surface tension gradients and, hence, the Marangoni flow hindering the film drainage. Distribution of the surfactant molecules (red head and dotted black tail) at the drop interface is schematic. The surfactant molecules inside the SDS drop are not shown. Green arrows indicate the interfacial and internal flows in the drop phase, induced by the surface tension gradient. Black arrows depict the flow distribution in the oil film beneath the drops.

the hydrodynamic force pushing the drops together [26]. Furthermore, we observe that the rupture occurs off-center in a ring round the rim, as it possibly has the minimum film thickness [27,36].

Since the Marangoni stress opposes film thinning, there is less surfactant at rupture near the contact line than elsewhere. Figure 2(c) illustrates that there is a transition time, about 200 ms, for the value of the exponent α to change from about 0.5 to about 1. The fact that α is less than 1 means that the thinning dynamics decelerates until the thinning evolves to $r \sim t$. The deceleration time constant is commensurate with the time constant of the dynamic surface tension, which is about 500 ms for SDS molecules, to be adsorbed at the interface and saturate it, which is shown in Fig. 1(c). Free surfactant molecules in the bulk of the drop migrate to the interface, tending to homogenize the surfactant concentration and, thus, relaxing the Marangoni stress. Hence, the spreading dynamic is changed in approximately 200 ms to the viscous regime, as depicted in Fig. 2(a).

IV. CONCLUDING REMARKS AND OUTLOOK

Summarizing, we studied the role of surfactants on the early-time dynamics of drop spreading. Two such spreading regimes are distinguished when the SDS surfactant at concentrations larger than 0.1 CMC is added to the system: (i) a retardation regime with $r \sim t^{0.5}$, and (ii) a viscous regime described by $r \sim t$. The Marangoni stress triggered by the nonuniform surfactant distribution at the drop interface is responsible for the change in the spreading dynamics. The retardation continues until adsorption of the surfactant at the interface smoothens the surface tension gradient. The relatively short-time dynamics reduces considerably the spreading velocity and, hence, extends the total wetting time by 1 order of magnitude. The characteristics of an aqueous drop spreading on solids, in terms of the velocity and the extent of the wetting, are the keys to many deposition processes, including coating, printing, enhanced oil production, and surfactant replacement therapies. Our discovery establishes a guideline for future numerical and analytical studies of drop spreading in the presence of surface-active materials. Furthermore, it can be used to distinguish the presence of surface-active molecules and particles in terms of impurities in the relevant processes.

ACKNOWLEDGMENTS

We thank Dr. George M. (Bud) Homsy (Washington State University) for numerous fruitful and enlightening discussions and comments during the course of this work. We acknowledge Dr. Muhammad Sahimi (University of Southern California) for reviewing and help in writing the manuscript. Financial support from the Natural Sciences and Engineering Research Council of Canada (NSERC) under Discovery Grant No. 07186-2019, the Alberta Innovates Graduate Student

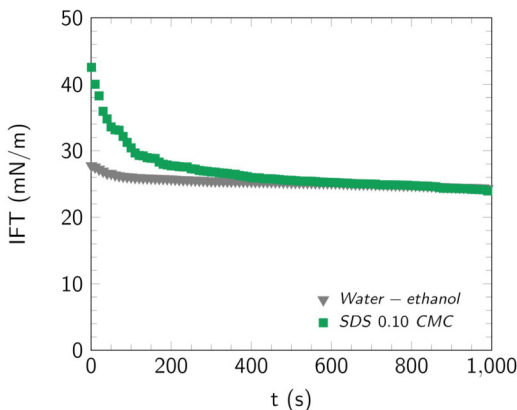


FIG. 5. Dynamic IFT of the SDS 0.1 CMC droplet and the water-ethanol droplet in the surrounding oil phase. The IFT of the water-ethanol droplet remains constant over time. However, the IFT of the SDS 0.1 CMC droplet is a function of time. Both systems have the same equilibrium IFT.

Scholarships, and the University of Calgary Eyes High Doctoral program is highly appreciated. The authors also gratefully acknowledge infrastructure funding from the Canadian Foundation for Innovation (CFI) under CFI LOF Project No. 30100.

APPENDIX A: COMPARING INTERFACIAL TENSION OF WATER-ETHANOL SOLUTION AND SDS SOLUTION

Figure 5 shows a comparison of the interfacial tension of the water-ethanol solution and the SDS solution.

APPENDIX B: EFFECT OF DROP VOLUME AND SURROUNDING LIQUID VISCOSITY ON THE INITIAL REGIME OF SURFACTANT DROP SPREADING

We observe the retarding effect of surfactants for different drop sizes and also different surrounding liquid viscosities. Figure 6 shows the effect of drop size and viscosity. For the drop

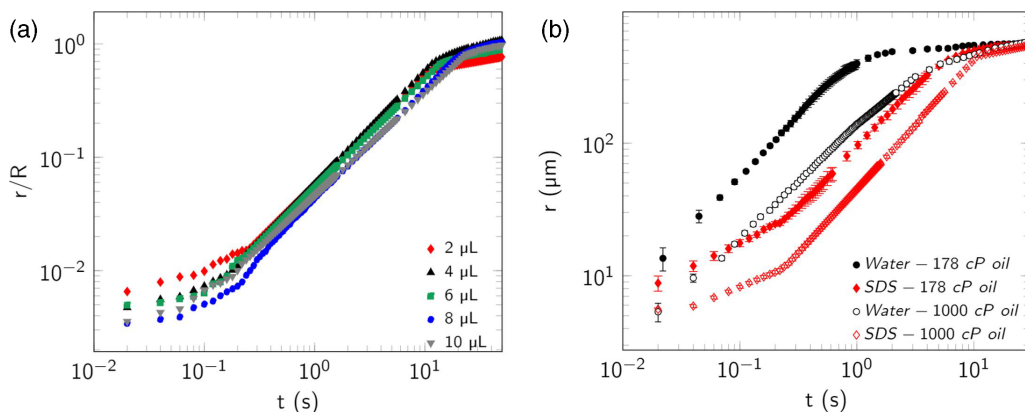


FIG. 6. (a) Effect of initial drop volume on the spreading regimes. A 1 CMC solution of SDS drop spreading (scaled with the initial drop radius) with different volumes from 2 to 10 μl . (b) Effect of the surrounding liquid viscosity on spreading regimes.

volume used, the transition between the two regimes does not depend on the drop size and the surrounding liquid viscosities.

-
- [1] D. Bonn, J. Eggers, J. Indekeu, J. Meunier, and E. Rolley, Wetting and spreading, *Rev. Mod. Phys.* **81**, 739 (2009).
 - [2] P. G. de Gennes, X. Hua, and P. Levinson, Dynamics of wetting: Local contact angles, *J. Fluid Mech.* **212**, 55 (1990).
 - [3] J. E. Sprittles, Kinetic Effects in Dynamic Wetting, *Phys. Rev. Lett.* **118**, 114502 (2017).
 - [4] J. Ro and G. Homsy, Viscoelastic free surface flows: Thin film hydrodynamics of Hele-Shaw and dip coating flows, *J. Non-Newtonian Fluid Mech.* **57**, 203 (1995).
 - [5] Q. Yuan and Y.-P. Zhao, Precursor Film in Dynamic Wetting, Electrowetting, and Electro-Elasto-Capillarity, *Phys. Rev. Lett.* **104**, 246101 (2010).
 - [6] C. Leuner and J. Dressman, Improving drug solubility for oral delivery using solid dispersions, *Eur. J. Pharm. Biopharm.* **50**, 47 (2000).
 - [7] J. de Coninck, M. J. de Ruijter, and M. Voué, Dynamics of wetting, *Curr. Opin. Colloid Interface Sci.* **6**, 49 (2001).
 - [8] A. Eddi, K. G. Winkels, and J. H. Snoeijer, Short time dynamics of viscous drop spreading, *Phys. Fluids* **25**, 013102 (2013).
 - [9] S. Mitra and S. K. Mitra, Understanding the early regime of drop spreading, *Langmuir* **32**, 8843 (2016).
 - [10] H. de Maleprade, C. Clanet, and Quéré, Spreading of Bubbles after Contacting the Lower Side of an Aerophilic Slide Immersed in Water, *Phys. Rev. Lett.* **117**, 094501 (2016).
 - [11] P. Bazazi, A. Sanati-Nezhad, and S. H. Hejazi, Wetting dynamics in two-liquid systems: Effect of the surrounding phase viscosity, *Phys. Rev. E* **97**, 063104 (2018).
 - [12] L. Tanner, The spreading of silicone oil drops on horizontal surfaces, *J. Phys. D: Appl. Phys.* **12**, 1473 (1979).
 - [13] M. J. de Ruijter, J. De Coninck, and G. Oshanin, Droplet spreading: Partial wetting regime revisited, *Langmuir* **15**, 2209 (1999).
 - [14] M. J. De Ruijter, M. Charlot, M. Voué, and J. De Coninck, Experimental evidence of several time scales in drop spreading, *Langmuir* **16**, 2363 (2000).
 - [15] M. Fermigier and P. Jenffer, An experimental investigation of the dynamic contact angle in liquid-liquid systems, *J. Colloid Interface Sci.* **146**, 226 (1991).
 - [16] S. Goossens, D. Seveno, R. Rioboo, A. Vaillant, J. Conti, and J. De Coninck, Can we predict the spreading of a two-liquid system from the spreading of the corresponding liquid-air systems? *Langmuir* **27**, 9866 (2011).
 - [17] D. Seveno, T. D. Blake, S. Goossens, and J. De Coninck, Predicting the wetting dynamics of a two-liquid system, *Langmuir* **27**, 14958 (2011).
 - [18] T. D. Blake and J. M. Haynes, Kinetics of liquid/liquid displacement, *J. Colloid Interface Sci.* **30**, 421 (1969).
 - [19] A. D. Nikolov, D. T. Wasan, A. Chengara, K. Koczó, G. A. Policello, and I. Kolossvary, Superspreading driven by Marangoni flow, *Adv. Colloid Interface Sci.* **96**, 325 (2002).
 - [20] S. Rafai, D. Sarker, V. Bergeron, J. Meunier, and D. Bonn, Superspreading: Aqueous surfactant drops spreading on hydrophobic surfaces, *Langmuir* **18**, 10486 (2002).
 - [21] X. Wang, L. Chen, E. Bonaccorso, and J. Venzmer, Dynamic wetting of hydrophobic polymers by aqueous surfactant and superspreader solutions, *Langmuir* **29**, 14855 (2013).
 - [22] D. T. Wasan and A. D. Nikolov, Spreading of nanofluids on solids, *Nature (London)* **423**, 156 (2003).
 - [23] M. Filoche, C.-F. Tai, and J. B. Grotberg, Three-dimensional model of surfactant replacement therapy, *Proc. Natl. Acad. Sci. USA* **112**, 9287 (2015).
 - [24] M. J. Rosen and J. T. Kunjappu, *Surfactants and Interfacial Phenomena* (Wiley, New York, 2012).

- [25] Z. Niroobakhsh, J. A. LaNasa, A. Belmonte, and R. J. Hickey, Rapid Stabilization of Immiscible Fluids Using Nanostructured Interfaces via Surfactant Association, *Phys. Rev. Lett.* **122**, 178003 (2019).
- [26] B. Dai and L. G. Leal, The mechanism of surfactant effects on drop coalescence, *Phys. Fluids* **20**, 040802 (2008).
- [27] L. Y. Yeo, O. K. Matar, E. S. P. de Ortiz, and G. F. Hewitt, The dynamics of Marangoni-driven local film drainage between two drops, *J. Colloid Interface Sci.* **241**, 233 (2001).
- [28] K. L. Pan, Y. H. Tseng, J. C. Chen, K. L. Huang, C. H. Wang, and M. Lai, Controlling droplet bouncing and coalescence with surfactant, *J. Fluid Mech.* **799**, 603 (2016).
- [29] W. H. Weheliye, T. Dong, and P. Angeli, On the effect of surfactants on drop coalescence at liquid/liquid interfaces, *Chem. Eng. Sci.* **161**, 215 (2017).
- [30] Hsien-Hung Wei, Marangoni-enhanced capillary wetting in surfactant-driven superspreading, *J. Fluid Mech.* **855**, 181 (2018).
- [31] N. Kovalchuk, A. Barton, A. Trybala, and V. Starov, Surfactant enhanced spreading: Catanionic mixture, *Colloids Interface Sci. Commun.* **1**, 1 (2014).
- [32] G. Karapetsas, R. V. Craster, and O. K. Matar, On surfactant-enhanced spreading and superspreading of liquid drops on solid surfaces, *J. Fluid Mech.* **670**, 5 (2011).
- [33] T. Roques-Carnes, V. Mathieu, and A. Gigante, Experimental contribution to the understanding of the dynamics of spreading of Newtonian fluids: Effect of volume, viscosity and surfactant, *J. Colloid Interface Sci.* **344**, 180 (2010).
- [34] M. von Bahr, F. Tiberg, and V. Yaminsky, Spreading dynamics of liquids and surfactant solutions on partially wettable hydrophobic substrates, *Colloids Surf., A* **193**, 85 (2001).
- [35] F. Baldessari, G. Homsy, and L. G. Leal, Linear stability of a draining film squeezed between two approaching droplets, *J. Colloid Interface Sci.* **307**, 188 (2007).
- [36] B. Liu, R. Manica, and Q. Liu, Coalescence of bubbles with mobile interfaces in water, *Phys. Rev. Lett.* **122**, 194501 (2019).